

for 2β and for

$$S(V_c) = \left\{ \sum_V w(V) (I_B^m(V) - c(V_c - V)^{2\beta})^2 \right\}^{1/2}$$

are shown in Fig. 3. It is concluded that $2\beta = 0.618$ with an estimated uncertainty of ± 0.010 and $V_c = 19\,166.5 \mu\text{V}$. In Fig. 4 is shown I_B^m versus $V_c - V$ in a double log plot, and at the top of Fig. 4 is shown the difference δ between the measured intensities and the least-squares fit relative to the standard deviation of I_B^m . It is concluded that (8) fits the data satisfactorily.

Similar measurements were carried out for (1,0,0) and (1,1,1) reflections in the parallel orientation and results were, respectively, $(2\beta, V_c) = (0.592, 19\,167.6 \mu\text{V})$ and $(2\beta, V_c) = (0.593, 19\,168.6 \mu\text{V})$. In a double log plot like Fig. 4 no deviation from a straight line was apparent down to temperatures 25° below T_c .

The consistency of these three sets of data give confidence to the assertion:

$$\beta = 0.305 \pm 0.005.$$

CONCLUSION

The temperature dependence of long-range order in the vicinity of the critical temperature T_c has been deduced from the temperature dependence of the peak intensity from a superlattice reflection. It is essential for proper interpretation of the data that extinction is negligible; in the present work this was obtained by

using a small sample (2-mm thickness) at medium wavelength (1.56 Å). Consistent results were found from the (1,1,1) and (1,0,0) reflections in the parallel and the antiparallel orientations. Background count rate due to critical scattering was subtracted and the resulting intensity I_B obeyed the power law $I_B \propto (T_c - T)^{2\beta}$ with $\beta = 0.305 \pm 0.005$, in agreement with the prediction of the Ising model. Values of β found in magnetic systems are generally slightly greater than the value we observed for the alloy, and this might indicate a small difference between a Heisenberg and an Ising magnet as regards the temperature dependence of long-range order.

The neutron-diffraction method can in principle also be used to determine the temperature dependence of the susceptibility and the correlation range of short-range order below T_c . Unfortunately the accuracy suffers seriously by the superposition of a Bragg peak on the critical scattering. We have determined the square of the ratio between the inverse correlation ranges ΔT below and above T_c and found $(\kappa_1^-/\kappa_1^+)^2 = 8.5 \pm 3.0$ at $\Delta T = 2.1^\circ$ and $(\kappa_1^-/\kappa_1^+)^2 = 5.5 \pm 2.0$ at $\Delta T = 4.4^\circ$. The prediction of the Ising model is $(\kappa_1^-/\kappa_1^+)^2 = 5.2$ independent of mT . Improvement of the accuracy for critical scattering below T_c would be of considerable interest and may be obtained with a crystal enriched with Cu⁶⁵.

Fermi Surface of Pb under Hydrostatic Pressure*

J. R. ANDERSON

University of Maryland, College Park, Maryland

AND

W. J. O'SULLIVAN AND J. E. SCHIRBER

Sandia Laboratory, Albuquerque, New Mexico

(Received 17 June 1966; revised manuscript received 1 August 1966)

Measurements of the effect of hydrostatic pressure on the Fermi surface of lead are reported. The frequencies of the α , β , and γ oscillations were all found to increase by about 0.3% kbar^{-1} , a rate more than twice that expected from scaling of the Fermi surface with volume. The pressure results on the β oscillations provide evidence for the association of these oscillations with the ν orbit. Estimates of the variations with pressure of the Fourier coefficients of the pseudopotential are obtained, as well as estimates of the average values of the diagonal components of Pippard's deformation parameter for the three orbits. Our results suggest that simple pseudopotential-model calculations can give at best a qualitative estimate of the potential change resulting from small variations of the wave vectors with pressure.

INTRODUCTION

THE de Haas-van Alphen (dHvA) effect has been used by Anderson and Gold¹ to determine the Fermi surface of lead. Although a reasonable description was obtained, there was some uncertainty in the assign-

ment to a particular section of the Fermi surface of the very strong β oscillations. These oscillations were attributed to an electron orbit ν in the third band formed by the intersection of four {110} "arms" (Fig. 1), which was by far the most reasonable choice, but a second possibility was to assign the oscillations to a third-band hole orbit ξ lying in the square face of the Brillouin zone. Pressure studies provide additional evi-

* Supported in part by the U. S. Atomic Energy Commission and by the Advanced Research Projects Agency.

¹ J. R. Anderson and A. V. Gold, Phys. Rev. **139**, 1459 (1965).

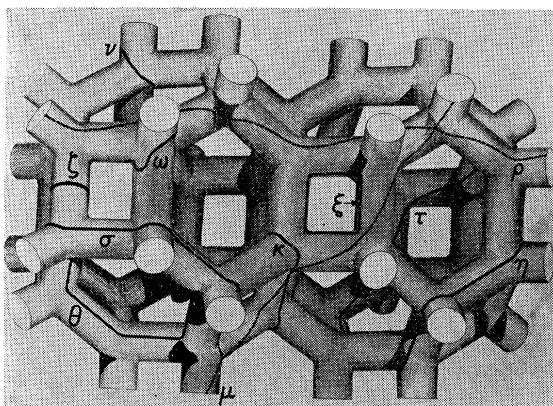


FIG. 1. A portion of the 4-parameter electron surface in the third zone (schematic).

dence for association of the β oscillations with orbit ν . In addition, pressure studies have been made of the α and γ oscillations for $H \parallel [110]$. The α oscillations are attributed to the second-zone hole surface (orbit ψ) while the γ oscillations are attributed to orbit ζ around the $\{110\}$ third-band "arms" (Fig. 1).

Estimates have been obtained of changes with pressure in the four orthogonalized-plane-wave (OPW) fitting parameters used by Anderson and Gold.¹ The results indicate that the pressure shifts of the V_{111} and V_{200} parameters are greater by roughly a factor of 4 than predicted by the simple application of a model pseudopotential.² This report describes these results and the pressure measurement techniques.

EXPERIMENTAL PROCEDURE

Samples used in this experiment were cut by spark erosion from a 5-9's pure lead single crystal and were roughly rectangular in cross section (0.25 cm on a side and about 1 cm long). From earlier work³ on crystals from the same ingot, the residual resistance ratio $\rho_{300^\circ\text{K}}/\rho_{4.2^\circ\text{K}}$ of these samples is approximately 10^4 . These samples were inserted in a beryllium-copper bomb with circular cross section ($\frac{1}{8}$ -in. i.d., $\frac{7}{16}$ -in. o.d.). In order to prevent motion during pressure changes, the samples were slip-fit into copper helices which made fairly close contact with the walls of the bomb. In addition, all measurements were made for the magnetic field along symmetry directions where dHvA periods vary slowly with orientation.

The pressure technique has been described previously by Schirber.⁴ Figure 2 shows a schematic of this pressure apparatus. Since the pressure transmitting medium is solid helium, it is necessary to raise the sample holder out of the cryostat to allow the helium to melt before

the pressure can be varied. The sample-holder is then lowered slowly into the cryostat while the pressure is maintained approximately constant and the helium allowed to solidify starting at the bottom. A copper-constantan thermocouple is used to monitor the temperature during this procedure. The final pressure can be determined from the equation of state⁵ assuming that cooling is essentially at constant volume below the solidification temperature ($<30^\circ\text{K}$). Generally, zero pressure dHvA signals were not noticeably changed after cycling to 4 kbars. Templeton⁶ has studied pressure effects in the noble metals using another approach based upon the fact that at 1°K helium remains liquid up to pressures of 25 atm. He measures the relative phase changes occurring while the pressure is varied continuously. This method has the advantages of speed and simplicity, but complicated patterns such as those observed in Pb produce phase changes which are difficult to interpret.

The conventional field-modulation technique used by Shoenberg and Stiles⁷ was slightly modified for this study. The usual modulation frequency was 200 cps and standard phase-sensitive detection methods were used to detect the fundamental and second-harmonic signals picked up from the sample. The magnetic field was produced by a 55-kG Westinghouse superconducting magnet with uniformity of better than 1 part in 10^4 over a $\frac{1}{2}$ -in. sphere. The modulation coil (5 in. long layer of 40 A.W.G. wire) was wound inside the vacuum space of the tail of the helium Dewar insert. The compensated pickup coil was made up of two parts wound in opposition. Each part contained approximately 5000 turns of No. 46 wire. This coil fitted snugly over the bomb.

Because the bomb had to be warmed above the freezing point of He in order to change the pressure, it was necessary to make accurate period measurements over the same field range at several pressures. With

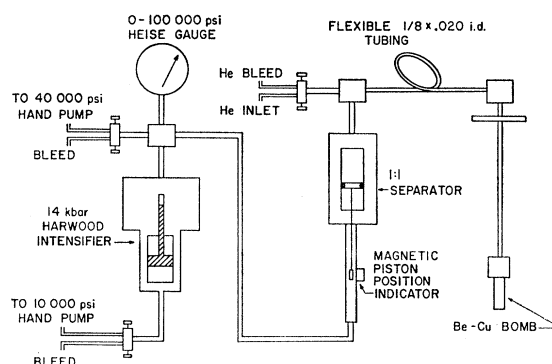


FIG. 2. Schematic of the 5-kbar solid-helium pressure apparatus.

² W. A. Harrison, *Phys. Rev.* **131**, 2433 (1963); *Rev. Mod. Phys.* **36**, 256 (1964).

³ J. E. Schirber, *Phys. Rev.* **131**, 2459 (1963).

⁴ J. E. Schirber, in *Physics of Solids at High Pressures*, edited by C. T. Tomizuka and R. F. Emrick (Academic Press Inc., New York, 1965); *Phys. Rev.* **140**, A2061 (1965).

⁵ J. S. Dugdale, in *Physics of High Pressures in the Condensed State*, edited by A. van Itterbeek (North-Holland Publishing Company, Amsterdam, 1965).

⁶ I. M. Templeton, *Proc. Roy. Soc. (London)* **292**, 413 (1966).

⁷ D. Shoenberg and P. J. Stiles, *Proc. Roy. Soc. (London)* **281**, 62 (1964).

measurements of ~ 200 dHvA cycles, it was possible to determine relative periods to perhaps 0.05% if there were no complications due to mixing of several periods. However, in order to make measurements of this precision it was necessary to take the inductive hysteresis and the frozen-in flux in the superconducting magnet into account. Measurement of current through the magnet might give errors in the field values of 50–100 G. Therefore, a copper wire magnetoresistance probe was used to check that period measurements were made over the same field range and in this manner the field could be reproduced to within 10 G.

RESULTS

The α and γ oscillation frequencies for H parallel to $[110]$ and the β oscillation frequencies for H parallel to $[100]$ were measured as a function of pressure and the results are shown in Fig. 3. From the sound velocity measurements of Waldorf and Alers,⁸ the volume compressibility of lead is $K_T = 2.05 \times 10^{-3}/\text{kbar}$ at 4°K. If the changes in dHvA frequencies followed only from the changes in lattice constant due to compressibility, the result would be

$$(1/F)(dF/dP) = -\frac{2}{3}K_T, \quad (1)$$

where F is the dHvA frequency and P is the pressure. This result is plotted as the dashed line in Fig. 3 and we see that the experimental changes are roughly twice the magnitude predicted by the decrease in lattice constant alone.

The dHvA frequencies are proportional to extremal cross-sectional areas \mathcal{A} of the Fermi surface which have been calculated in Ref. 1. At zero pressure the relationship becomes $\mathcal{A}_0 = 5.8 \times 10^{-9} F_0$ where \mathcal{A}_0 is the area in units of $(2\pi/a)^2$, F_0 is the frequency in gauss, and the lattice constant a is estimated to be 4.90×10^{-8} cm.⁹ The experimental results are

$$\frac{1}{\mathcal{A}} \left(\frac{\partial \mathcal{A}}{\partial P} \right)_{\alpha} = (3.1 \pm 0.4) \times 10^{-3}/\text{kbar},$$

$$\frac{1}{\mathcal{A}} \left(\frac{\partial \mathcal{A}}{\partial P} \right)_{\beta} = (2.7 \pm 0.4) \times 10^{-3}/\text{kbar},$$

$$\frac{1}{\mathcal{A}} \left(\frac{\partial \mathcal{A}}{\partial P} \right)_{\gamma} = (2.4 \pm 0.6) \times 10^{-3}/\text{kbar}.$$

The larger error estimate for the γ oscillations results from the apparent mixing of the α and γ oscillations and the long beats in the γ oscillations.¹ Filtering and differentiating the output of the phase-sensitive detector was only partially successful in reducing these effects.

In Ref. 1 the cross-sectional areas of the Fermi surface are given in terms of four parameters E_F , V_{111} , V_{200} , and λ . The Fermi energy E_F is determined by the restriction that the number of electrons removed from

⁸ D. L. Waldorf and G. A. Alers, J. Appl. Phys. 33, 3266 (1962).

⁹ G. K. White, Phil. Mag. 7, 271 (1962).

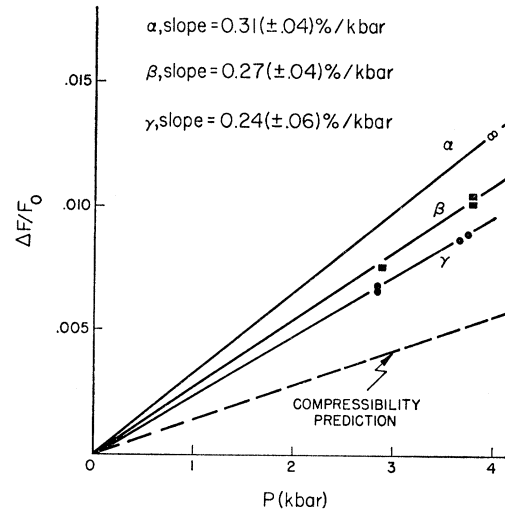


Fig. 3. The pressure dependence of the α , β , and γ dHvA frequencies of Pb. $\Delta F \equiv F(P) - F_0$, where $F(P)$ is the dHvA frequency at pressure P and F_0 the frequency at $P=1$ bar.

the second zone equals the number of electrons in the third zone. The parameters V_{111} and V_{200} are Fourier components of the pseudopotential while λ is the spin-orbit parameter which is approximately given by the atomic value. Since the areas are calculated in units of $(2\pi/a)^2$, one can write

$$\mathcal{A} = (2\pi/a)^2 \mathcal{A}_0(E_F, V_{111}, V_{200}, \lambda). \quad (2)$$

Therefore, one obtains for the relative change of area with pressure

$$\frac{1}{\mathcal{A}} \frac{d\mathcal{A}}{dP} = \frac{2}{3}K_T + \frac{1}{\mathcal{A}_0} \left(\frac{\partial \mathcal{A}_0}{\partial E_F} \frac{\partial E_F}{\partial P} + \frac{\partial \mathcal{A}_0}{\partial V_{111}} \frac{\partial V_{111}}{\partial P} + \frac{\partial \mathcal{A}_0}{\partial V_{200}} \frac{\partial V_{200}}{\partial P} + \frac{\partial \mathcal{A}_0}{\partial \lambda} \frac{\partial \lambda}{\partial P} \right). \quad (3)$$

With the procedures of Ref. 1, the derivatives of \mathcal{A}_0 have been calculated and are given in Table I. (The zero pressure values of the parameters¹ are, in rydbergs, $V_{111} = -0.084 \pm 0.002$, $V_{200} = -0.039 \pm 0.002$, $E_F = 0.718 \pm 0.001$, and $\lambda = 0.096 \pm 0.002$.)

Since the main contribution to λ comes from the atomic-core region, we assume that the pressure dependence of λ is dominated by effects due to renormalization of the wavefunction with the compression of

TABLE I. Derivatives of extremal areas of cross section.

Orbit	$\frac{\partial \ln \mathcal{A}_0}{\partial \ln E_F}$	$\frac{\partial \ln \mathcal{A}_0}{\partial \ln V_{111}}$	$\frac{\partial \ln \mathcal{A}_0}{\partial \ln V_{200}}$	$\frac{\partial \ln \mathcal{A}_0}{\partial \ln \lambda}$
	$\psi[110]$	-2.8	-0.07	-0.025
$\nu[100]$	8.91	0.025	-0.27	-0.26
$\zeta[110]$	10.35	-0.50	-0.13	-0.32

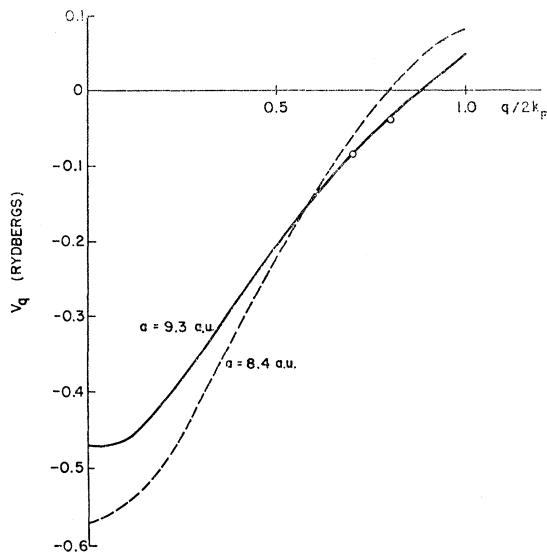


FIG. 4. Model potential form factors for lead (Ref. 2) calculated for a β of 46 Ry-(a.u.)³. The solid line shows the results for the normal lattice spacing and the dashed line represents a 10% decrease in lattice spacing. The circles represent the 4-parameter values for the normal lattice spacing.

the unit cell¹⁰ (i.e., $\partial\lambda/\partial P = -K_T\lambda_0 \approx -1.9 \times 10^{-4}$ Ry/kbar). With this assumption,¹¹ pressure changes in the two Fourier coefficients as well as the Fermi energy can be determined from the data. The results are

$$\frac{1}{E_F} \frac{\partial E}{\partial P} \approx -0.044 \times 10^{-2} / \text{kbar},$$

$$\frac{1}{V_{111}} \frac{\partial V_{111}}{\partial P} \approx -0.58 \times 10^{-2} / \text{kbar}$$

and

$$\frac{1}{V_{200}} \frac{\partial V_{200}}{\partial P} \approx -1.8 \times 10^{-2} / \text{kbar}.$$

The corresponding absolute changes are $\partial E_F/\partial P \approx -3.2 \times 10^{-4}$ Ry/kbar, $\partial V_{111}/\partial P \approx 4.9 \times 10^{-4}$ Ry/kbar, and $\partial V_{200}/\partial P \approx 7.0 \times 10^{-4}$ Ry/kbar. The errors in these determinations are estimated to be about 25%.

The variation in V_{200} and V_{111} with pressure is seen to be quite large. This large change predicts a similar decrease with pressure of the energy level E_3 ,¹ which lies just below the Fermi level at the zone corner W , since $\partial E_3/\partial P = -\partial V_{200}/\partial P$.

In order to compare these experimental values with theoretical predictions we have plotted in Fig. 4 the form factor V_q obtained from Harrison's point-ion potential.² The value of β (the delta-function repulsive-

core parameter) for this model calculation has been taken as 46 Ry-(a.u.)³ (here a.u.=atomic unit of length) in order to fit the 4-OPW estimate of V_{111} (-0.084 Ry). In Fig. 4 are shown the results for both the normal lattice constant (4.90×10^{-8} cm) and for a lattice constant decreased by 10%. From this plot or from an explicit derivative of the expression for the point-ion form factor assuming constant β one obtains

$$\frac{1}{V_{111}} \frac{\partial V_{111}}{\partial P} = -0.13 \times 10^{-2} / \text{kbar}$$

and

$$\frac{1}{V_{200}} \frac{\partial V_{200}}{\partial P} = -0.5 \times 10^{-2} / \text{kbar}.$$

It can be seen that the signs of the pressure derivatives of V_{111} and V_{200} agree with the point-ion-model predictions, but the magnitudes of the experimental changes are roughly 4 to 5 times the theoretical estimates. The reasons for this difference are not known. Large discrepancies between the results of pressure dHvA studies on zinc¹² and the point-ion model predictions have also been observed. The lead results rely heavily upon the value for compressibility, but it is unlikely that errors in either this quantity or the dHvA pressure dependence are sufficient to explain this difference. These results might be used to predict the pressure dependence of the parameter β , but a rather large value [$(1/\beta)(\partial\beta/\partial P) \approx 3 \times 10^{-3} / \text{kbar}$] would be required. Although there are no calculations for different atomic volumes in lead, Harrison¹³ has compared the computed form factor using the full theory with the point-ion results at two densities in aluminum. From this comparison one would predict $(1/\beta)(\partial\beta/\partial P) \approx 5 \times 10^{-5} / \text{kbar}$ for aluminum. Thus it is unlikely that the relaxation of the requirement that β be constant under pressure changes would have much physical significance. Detailed calculations for lead similar to those for aluminum and including the effects of spin-orbit coupling¹⁴ would be desirable in order to check this point. Calculations with the Heine-Abarenkov model potential¹⁵ are presently being carried out in order to study the pressure dependence of the lead form factors.

From these pressure measurements it is also possible to obtain average values of diagonal components of the deformation parameter described by Pippard.¹⁶ If Δk_N is the normal displacement of the Fermi surface in the direction of increasing energy produced by the strain $\bar{\omega}_{ij}$, the deformation parameter K_{ij} is defined by

$$\Delta k_N = \sum_{i,j} K_{ij} \bar{\omega}_{ij}. \quad (4)$$

¹² W. J. O'Sullivan and J. E. Schirber, Phys. Rev. **151**, 484 (1966).

¹³ W. A. Harrison, *Pseudopotentials in the Theory of Metals* (W. A. Benjamin, Inc., New York, 1966), pp. 33, 204.

¹⁴ A. O. E. Animalu, Phil. Mag. **13**, 53 (1966).

¹⁵ A. O. E. Animalu, Phil. Mag. **11**, 379 (1965).

¹⁶ A. B. Pippard, in *Low Temperature Physics*, edited by C. DeWitt, B. Dreyfus, and P. G. DeGennes (Gordon and Breach, Science Publishers, Inc., New York, 1961).

¹⁰ D. Brust and L. Liu, Solid State Commun. **4**, 193 (1966).

¹¹ The results for the pressure derivatives of the Fermi energy and the pseudopotential form factors are relatively insensitive to the details of this assumption. If we assume that $\partial\lambda/\partial P = 0$, the relative pressure changes of E_F , V_{111} , and V_{200} are increased in magnitude by about 15%. This difference is well within our experimental uncertainty.

TABLE II. Deformation parameter values in units of $(2\pi/a)$.

Orbit	k_l	$\langle K' \rangle_l$	$\langle K' \rangle_l / \langle K' \rangle_l^{sc}$
$\psi[110]$	4.8	0.40	2.3
$\nu[110]$	2.6	0.158	2.0
$\zeta[110]$	1.2	0.103	1.8

The pressure dependence of the dHvA frequency measures the change in area

$$\Delta\mathcal{A} = \oint dk_i dk_n, \quad (5)$$

where dk_n is the displacement normal to the orbit and to the magnetic field produced by the hydrostatic pressure and the integral is taken around the orbit (dk_t is the increment in k tangent to the orbit). The displacement normal to the Fermi surface Δk_N can be related to dk_n by $dk_n = \Delta k_N (1 - V_H^2/V^2)^{1/2}$ where V is the velocity and V_H is the component parallel to the magnetic field. Since lead is cubic, we have for the case of hydrostatic pressure $\bar{\omega}_{ij} = \bar{\omega}_{11}\delta_{ij}$, and the equation for $\Delta\mathcal{A}$ becomes

$$\Delta\mathcal{A} = \oint dk_i \bar{\omega}_{11} (K_{11} + K_{22} + K_{33}) (1 - V_H^2/V^2)^{1/2} \quad (6)$$

for an electron surface. If we substitute the compressibility K_T into this expression, we find

$$\begin{aligned} \frac{1}{K_T} \frac{\partial \mathcal{A}}{\partial P} &= \left\langle \frac{1}{3} (K_{11} + K_{22} + K_{33}) \left(1 - \frac{V_H^2}{V^2} \right)^{1/2} \right\rangle k_l \\ &= \langle K' \rangle_l k_l, \end{aligned} \quad (7)$$

where $\langle K' \rangle_l$ is one third the value of the sum of three diagonal elements of the deformation parameter times the velocity expression $(1 - V_H^2/V^2)^{1/2}$ averaged around an orbit l , and k_l is the distance around this orbit. In Table II are shown values of k_l and $\langle K' \rangle_l$ in units of $2\pi/a$ for the orbits ψ , ν , and ζ . For orbits ψ and ζ , V_H is zero and $\langle K' \rangle_l$ is one third of the average of the diagonal elements of the deformation parameter $\langle K \rangle_l$. For only a scaling effect $\langle K' \rangle_l$ would have the value $\langle K' \rangle_l^{sc} = \frac{2}{3}\mathcal{A}/k_l$. The ratio $\langle K' \rangle_l / \langle K' \rangle_l^{sc}$ is included in the table

and as expected $\langle K' \rangle_l$ is approximately twice the scaling value.

In the calculations of Ref. 1 the possibility of associating the β oscillations with orbit ξ (Fig. 1) was discussed. From our pressure results we see that both the area corresponding to the γ oscillations and that corresponding to the β oscillations become larger with pressure more rapidly than predicted by the scaling due to compressibility. Thus, since the arm cross sections determined by the γ oscillations increase more rapidly than simple scaling, the area determined by orbit ξ , a hole enclosed by four such arms, should increase more slowly with pressure than compressibility scaling predicts if the arms increase uniformly as seems likely. This is definitely not the case for the area corresponding to the β oscillations; thus, our results support the validity of the original assignment to orbit ν .

CONCLUSIONS

We have seen that pressure measurements of the dHvA effect can be used to study the dependence of potentials and energy bands upon lattice constants. In general cubic materials are more useful for this purpose since, although the changes may be small, they are not overshadowed by the anisotropic compressibility effects occurring in noncubic materials. Although model potential calculations predict the signs of the changes in V_{111} and V_{200} with pressure, the predicted magnitudes are smaller by a factor of 4 or 5.

This result suggests that model pseudopotentials adjusted to fit the zero-pressure experimental form factors at a finite number of wave-vector values can give only a qualitative estimate of the potential change for small variations about the initial wave vectors. However, calculations using more exact forms for the potential are required for a satisfactory comparison of theory with experiment.

ACKNOWLEDGMENTS

We wish to thank Dr. E. D. Jones for his valuable experimental suggestions and Dr. V. Heine for a helpful discussion. Computer time was supported in part by the University of Maryland Computer Science Center.

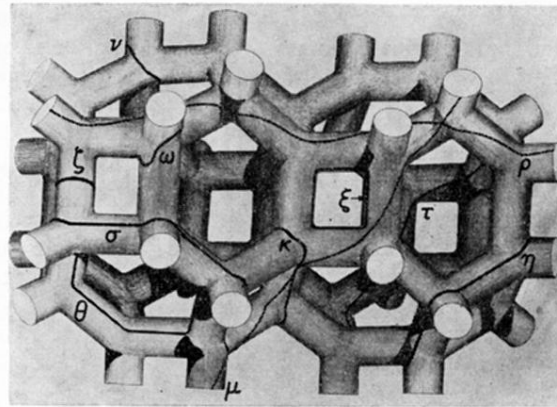


FIG. 1. A portion of the 4-parameter electron surface in the third zone (schematic).